Journal of Porphyrins and Phthalocyanines
J. Porphyrins Phthalocyanines 2001; **5**: 256–266

Excited states of four hemes in a c-type cytochrome subunit of the photosynthetic reaction center of *Rhodopseudomonas viridis*: SAC-CI calculations

K. OHKAWA,* M. HADA and H. NAKATSUJI

Department of Synthetic Chemistry and Biological Chemistry, Graduate School of Engineering, Kyoto University, Sakyo-ku, Kyoto 606-8501, Japan

Received 15 October 1999
Accepted 13 March 2000

ABSTRACT: The excited states of four hemes, c-552, c-554, c-556, and c-559, in a c-type cytochrome subunit of the photosynthetic reaction center (PSRC) of *Rhodopseudomonas (Rps.) viridis* were studied using the symmetry-adapted cluster (SAC)-configuration interaction (CI) method. c-552 has two imidazole ligands, while the other three hemes have imidazole and methionine ligands. The electronic states of these four hemes are affected significantly by both the ligands and protein and water environments. The ligand effect classifies the four hemes into two groups, while the environmental effect is unique in each heme. The HOMO–LUMO energy separation of c-552 is much smaller than those of the other hemes, and therefore, the low-lying excited states of c-552 are more stable than those of the other hemes. The low-lying excited states and their oscillator strengths of c-559 are significantly modified by the environment when compared with c-556 and c-554. Some observed UV peaks of the PSRC of *Rps. viridis* were found to have been assigned reasonably to the excited states of these four hemes in a previous report. The calculated linear dichroism angles also supported our assignment. Copyright © 2001 John Wiley & Sons, Ltd.

KEYWORDS: SAC-CI method; excited states; c-type cytochrome subunit; photosynthetic reaction center; linear dichroism (LD)

INTRODUCTION

Photosynthesis is an important biological process in which light is converted to chemical energy. The structure of the photosynthetic reaction center (PSRC) of *Rhodopseudomonas (Rps.) viridis* was determined by X-ray crystallography [1]. The PSRC consists of three hydrophobic H, L, and M subunits [2]. A c-type cytochrome subunit containing four hemes binds to this complex on the external side of the plasma membrane. These four hemes are identified by UV absorption peaks and other experimental methods [3–8] and are known as c-554, c-556, c-552, and c-559 according to the wavenumbers of their α-absorption bands.

An electron of an excited special pair (bacteriochlorophyll *b* dimmer) is passed through the L subunit containing bacteriochlorophyll *b* and bacteriopheophytin *b*, and reaches menaquinone and finally ubiquinone. The photo-oxidized special pair eventually regains its lost electron from the available redox carriers, which include membrane-spanning cytochrome bc_1 and cytochrome c_2 on the external side of the plasma membrane. In *Rps. viridis*, the four-heme c-type cytochrome subunit plays an important role in this electron transfer process, by being interposed between cytochrome c_2 and the special pair [1]. We believe that knowledge of the excited states of the c-type cytochrome subunit in the PSRC will provide a basic understanding of this electron transferring process.

Previously we theoretically studied the ground, excited, and ionized electronic states of various porphyrins [9–20] using the SAC (symmetry-adapted-cluster) [21] and SAC-CI (configuration interaction) [22–24] methods. These methods are known to accurately calculate various electronic states of a number of molecules [25, 26]. We first applied these methods to the electronic states of free-base porphin [9, 10] which is a basic molecule in a series of porphyrins. Then we applied these methods to magnesium porphin [11], iron porphyrin [13–15], tetrazaporphin [16], bacteriochlorin [12], pheophytin [12], and phthalocyanine [17]. The SAC and SAC-CI methods were an appropriate tool to investigate these relatively large compounds, and the calculated excitation energies and ionization energies agreed well with the experimental spectra of these porphyrin compounds. Recently, these methods were further applied to the photosynthetic reaction center of *Rhodopseudomonas (Rps.) viridis* to determine an assignment of its spectrum and clarify the mechanism of electron transfer [18–20].

In the present study, we applied the SAC and SAC-CI methods to study the excited states of four hemes, c-554, c-556, c-552, and c-559, in the c-type cytochrome subunit in the PSRC of *Rps. viridis*. The absorption spectra and linear dichroism (LD) spectra of the PSRC in *Rps. viridis* have been already observed [27] and we assigned these absorption peaks to the calculated excited states. We also discussed the nature of the excited states, particularly the origin of differences in the electronic structure of these four hemes mainly due to the differences in environmental

*Correspondence to: K. Ohkawa, Department of Synthetic Chemistry and Biological Chemistry, Graduate School of Engineering, Kyoto University, Sakyo-ku, Kyoto 606-8501, Japan.

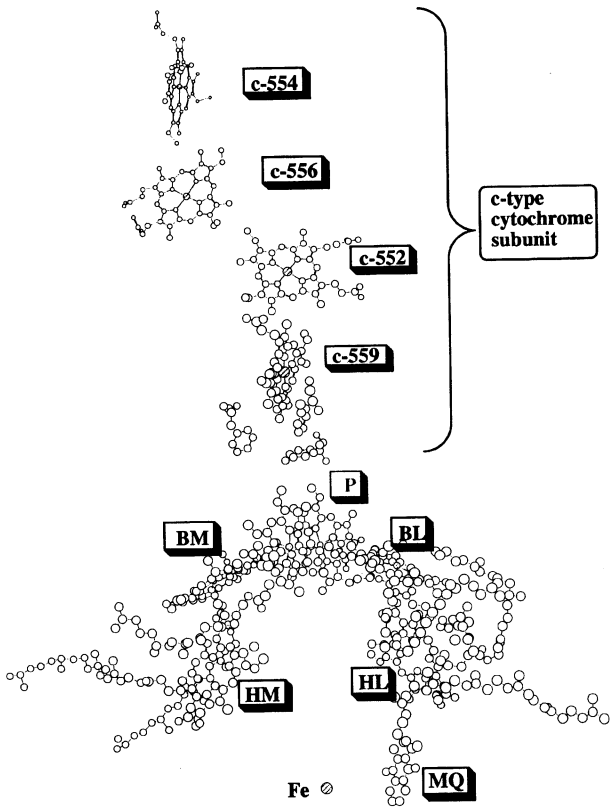

Fig. 1. Relative positions of chromophores and hemes in the PSRC of *Rps. viridis*. Four hemes are located in c-type cytochrome subunits (upper side) and several chromophores in L and M subunits.

effects and the ligands bound to Fe. The results of the present study have partially been utilized in the study of the absorption spectrum of the photosynthetic reaction center of *Rps. viridis* [18, 19].

COMPUTATIONAL DETAILS

The relative positions of chromophores and hemes in the PSRC of *Rps. viridis* are shown in Fig. 1. The four hemes, c554, c556, c552, and c559, are found in the c-type cytochrome unit, which is located above the complex of the L, M, and H subunits. An X-ray crystallographic structure was used to determine the geometries of these hemes, and therefore all hemes are treated without symmetry. The electronic wave functions are considered only for these four hemes, and the surrounding proteins and waters were replaced with the adequate point charges described below. To model the heme parts, some substituents which do not π-conjugate with the π-orbitals of the porphyrin ring are replaced with hydrogen atoms. Two vinyl groups directly bonded to the porphyrin ring are also replaced with hydrogen, since they π-conjugate with some neighboring aminoacids and not with porphyrin π-orbitals. The ligands of these hemes—histidine, aminoacid, and methionine—are replaced with imidazole and dimethylsulfide. The resultant model molecules are $[FeC_{26}N_8H_{18}]^{2-}$ for c-552 and $[FeC_{25}N_6SH_{21}]^{-}$ for c-554, c-556, and c-559. These model hemes are shown in Fig. 2. Only c-552 has two imidazoles, and the other hemes have imidazole and dimethylsulfide. The differences among the latter three

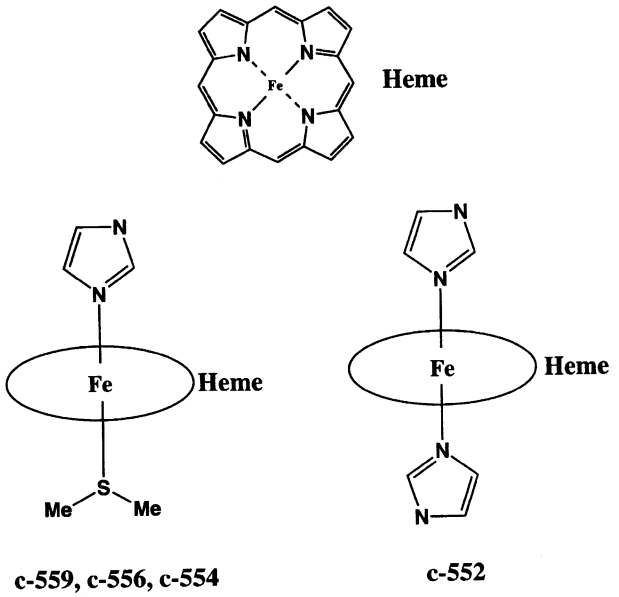

Fig. 2. Models of hemes in c-type cytochrome subunit in the PSRC.

hemes are attributed to differences in protein and water environments. Geometrical parameters also vary slightly from each other, since their structures are determined from X-ray data. Although the present simplified models are not fully satisfactory, we believe that they are acceptable because they have the essential characteristics of the three hemes.

Basis sets used for C and N were Huzinaga (63/41) [28, 29], and for H (4) [30]. The Huzinaga (5321/521) set augmented by p-function ($\zeta = 0.041$) and d-function ($\zeta = 0.421$) was used for S, and the Huzinaga (53321/53/41) set augmented by p-function ($\zeta = 0.082$) for Fe [28, 29]. The total number of SCF orbitals is 317 and 318, respectively, for c-552 and for c-559, c-556, and c-554.

The effect of proteins and waters, which collectively contain 30000 atoms, is introduced by the point charge model. Geometries of heavy atoms in the PSRC are taken from the X-ray structure (1PRC in Brookhaven Data Bank [31]). Positions of hydrogen atoms are estimated by using the molecular modeling software SYBYL [32]. To create the electrostatic field, amino acids were replaced with point charges used in AMBER [33], and all protein and water atoms were also replaced with point charges reported as TIP3P [34].

In the SAC and SAC-CI calculations, only the inner 1s core was frozen and 248 orbitals (94 occupied, 154 unoccupied orbitals) were utilized as active orbitals for c-552, while 246 orbitals (95 occupied, 151 unoccupied orbitals) were used for c-559, c-556, and c-553.

All single excitation operators were included in the linked term of the SAC and SAC-CI calculations, and perturbation selection was performed for double excitation operators. The energy threshold for perturbation selection was 2×10^{-5}.

The HONDO version 8 [35] program is used to carry out the Hartree–Fock SCF calculations, and the SAC85 [36] and SAC-CI96 [37, 38] programs are used to carry out the SAC and SAC-CI calculations

The linear dichroism (LD) spectrum calculated in the present study is expressed by the equation [39]

Table 1. Orbital energies and characters[a] of c-559, c556, c-554, and c-552 calculated in the gas phase and in the protein and water environment

	Gas phase		Proteins and waters	
Orbital number	Orbital energy (eV)	Orbital character	Orbital energy (eV)	Orbital character
		c-559		
Occupied				
125	−8.69	π(Por)	−11.22	π(Por)
126	−8.69	π(Por) + d_{z^2}(Fe)	−11.02	π(Por) + d_{z^2}(Fe)
127	−6.31	π(Por)	−9.10	π(Por)
128	−6.02	π(Por)	−8.77	π(Por)
Unoccupied				
129	0.54	π(Por)	−2.40	π(Por)
130	0.60	π(Por)	−2.02	π(Por)
131	3.22	π(Por)	0.56	π(Por)
132	3.57	3s(S) + 3s(Fe)	0.72	3s(S) + 3s(Fe)
		c-556		
Occupied				
125	−8.39	π(Por) + $d_{x^2-y^2}$(Fe)	−9.24	(Delocalized)
126	−7.99	π(Por) + $3p_z$(S)	−9.07	π(Por) + d_{z^2}(Fe)
127	−6.12	π(Por)	−6.96	π(Por)
128	−5.93	π(Por)	−6.59	π(Por)
Unoccupied				
129	0.44	π(Por)	−0.16	π(Por)
130	0.57	π(Por)	0.11	π(Por)
131	3.08	π(Por)	2.59	π(Por)
132	3.75	3s$3p_z$(S) + 3s(Fe)	2.72	2s(Fe) + π(Im)
		c-554		
Occupied				
125	−8.62	π(Por) + 3d(Fe) + $3p_y$(S)	−9.26	π(Por) $3p_z$(S)
126	−8.38	π(Por) + 3d(Fe)	−9.03	π(Por) + 3d(Fe)
127	−6.37	π(Por)	−7.11	π(Por)
128	−5.92	π(Por)	−6.69	π(Por)
Unoccupied				
129	0.60	π(Por)	−0.15	π(Por)
130	1.02	π(Por)	0.13	π(Por)
131	3.16	π(Im)	2.62	π(Im)
132	3.46	π(Por)	2.75	π(Por)
		c-552		
Occupied				
126	−8.86	π(Im) + $3d_{yz}$(Fe)	−10.96	π(Im) + π(Por)
127	−7.44	π(Por) + π(Im)	−10.63	π(Por) + π(Im)
128	−6.08	π(Por)	−9.38	π(Por)
129	−5.74	π(Por)	−9.05	π(Por)
Unoccupied				
130	−0.86	π(Por)	−4.20	π(Por)
131	0.42	π(Por)	−2.37	π(Por)
132	2.37	π(Por)	−0.89	π(Por)
133	3.83	π(Im)	0.88	π(Im) + π(Por)

[a] Por: porphyrin, Im: imidazole, S: sulfur of methionine.

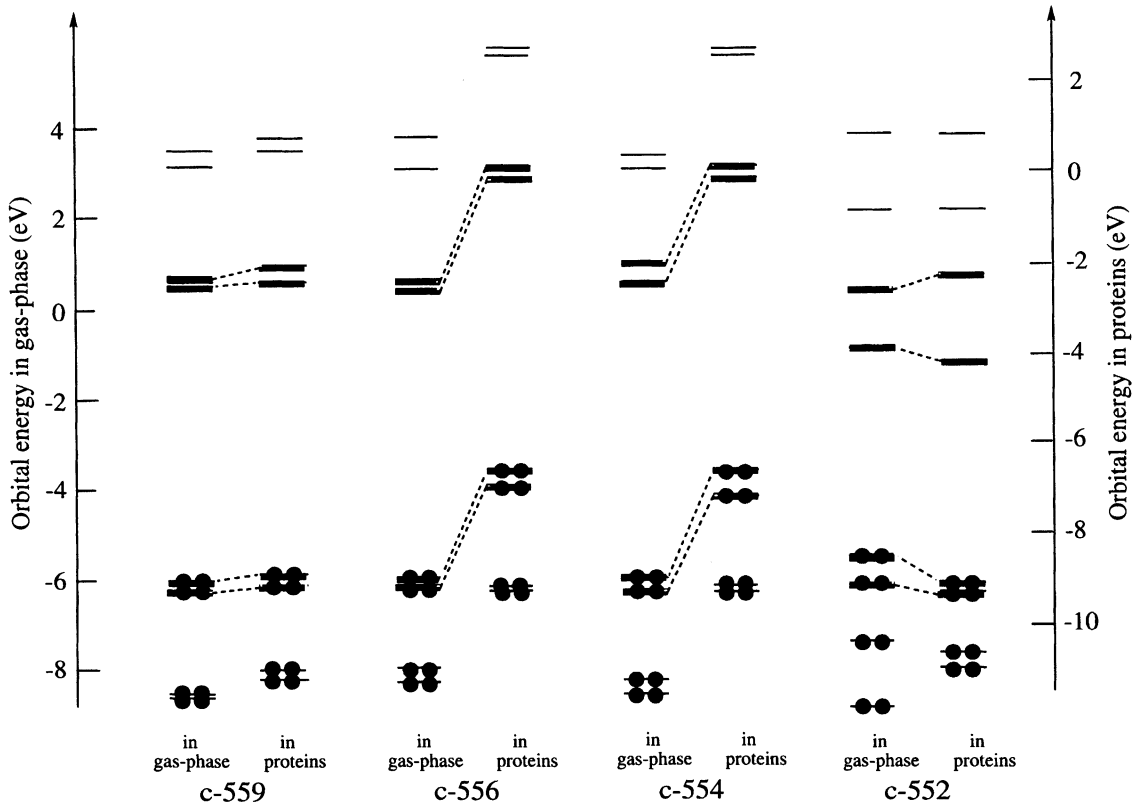

Fig. 3. Orbital energy diagrams of four hemes in the gas-phase and in proteins.

$$|\mu_{\perp}|^2 - |\mu_{\parallel}|^2 = (1 - \cos^2\theta)|\mu|^2 \qquad (1)$$

where θ is the angle between the transition moment μof the state and the pseudo C_2-axis. The $\perp$ and $\parallel$ in subscript denote parallel and perpendicular to the pseudo C_2-axis, respectively. The plus values correspond to $90° > \theta > 55°$, and the minus values correspond to $55° > \theta > 0°$.

GROUND STATES OF HEMES

Electronic ground states of c-559, c-556, c-554, and c-552 are closed-shell singlet states. Hartree–Fock orbital energies and orbital characters both in the gas phase and in the protein and water environment are listed in Table 1, and orbital energies are shown in Fig. 3. In c-559, c-556, and c-554, the so-called 'four orbitals' which consist of the highest occupied molecular orbital (HOMO), the next HOMO, the lowest unoccupied molecular orbitals (LUMO), and the next LUMO are well separated in energy from the other occupied and unoccupied orbitals, as clearly shown in Fig. 3. Gouterman's four-orbital model [40] appears to be a good zero-th order approximation of these three hemes. In c-552, however, the LUMO is stabilized and the next LUMO is destabilized by the replacement of methionine with imidazole. The environmental effect emphasizes this trend of c-552, and therefore Gouterman's four-orbital model cannot be applied to c-552.

The orbital characters of the four orbitals in proteins and waters themselves are essentially the same as those in the gas phase, whereas the characters of the other occupied and unoccupied orbitals are modified significantly. Orbital energies are significantly affected by electrostatic potential generated by the surrounding proteins and waters, and this effect is not uniform in the four hemes. The HOMO and the next HOMO in c-552 are stabilized by the environment, while the HOMOs are destabilized in the other hemes. The environmental effect particularly significantly destabilizes both occupied and unoccupied orbitals, as shown in Fig. 3.

Here we describe the difference between imidazole and methionine. Methionine's 3p(sulfur) orbital overlaps more with the porphyrin π-orbitals than the imidazole 2p(nitrogen) orbital does. This may cause destabilization of the HOMOs of c-559, c-556, and c554, which are localized at the N-atoms and exist as the next HOMO in c-552, FBP, and MgP.

Schematic pictures of the HOMO, the next HOMO, the LUMO, and the next LUMO of the four hemes are shown in Figs 4 and 5. All four orbitals are essentially π-orbitals on the porphyrin rings. In c-552 (Fig. 5), the next HOMO of c-552 is localized at the N-atoms and the *meso*-C atoms, and the HOMO is delocalized over the C atoms of the pyrole rings. In the other hemes (Fig. 4), the natures of these two orbitals are exchanged. We note here that the order of the HOMO and the next HOMO of c-552 is the same as that in free-base porphin (FBP) [9] and Mg-porphin (MgP) [11], while in the other hemes it is different from that in FBP and MgP. Since orbital order is essentially kept in both the gas phase and the protein environment, the difference in orbital order is not due to the effect of protein and water, but to the effect of the coordination of methionine binding to Fe.

The HOMO–LUMO (H–L) energy separations are listed in the upper half of Table 2. The HOMO–LUMO separations in proteins are 6.37–6.54 eV for c-559, c-556, and c-554, but it is much smaller (4.85 eV) in c-552. Furthermore, the HOMO–LUMO separations in c-559, c-556, and c-554 increase in the protein and water

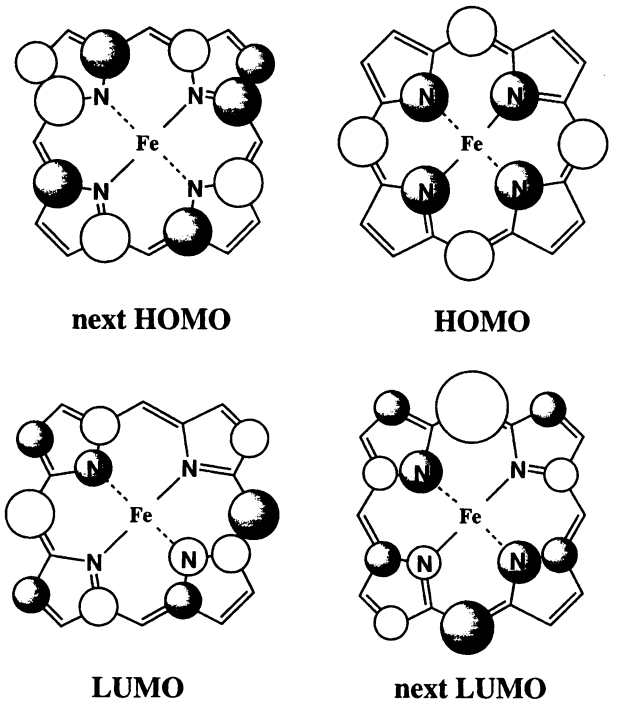

Fig. 4. Schematic representations of the next HOMO, HOMO, LUMO, and next LUMO of c-554, c-556, and c-559. These are top views of porphyrin p-orbitals.

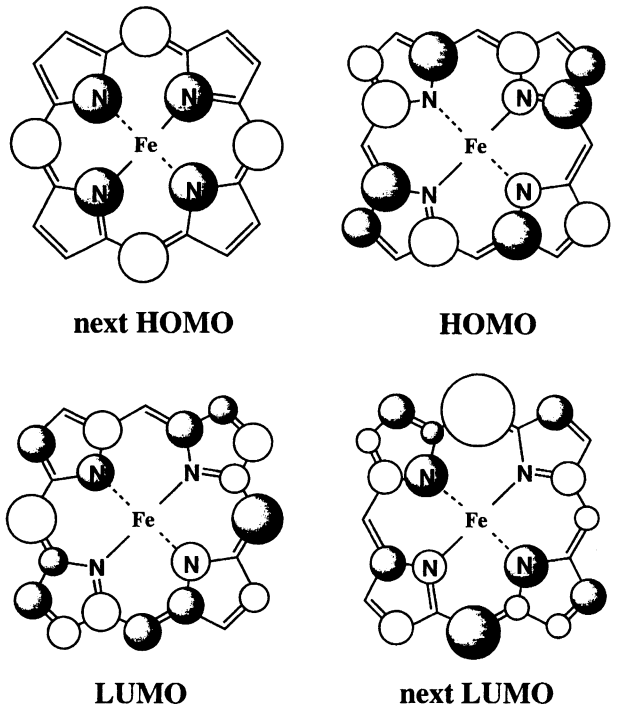

Fig. 5. Schematic representations of the next HOMO, HOMO, LUMO, and next LUMO of c-552. These pictures are top views of porphyrin p-orbitals.

environment, while it decreases in c-552. These facts strongly affect the excitation energies and oscillator strengths, as described in the next section.

EXCITED STATES OF HEMES

Tables 3–6 show the singlet excitation energies including

Table 2. Comparisons of energy separations between the HOMO and the LUMO and summary of low-lying excitation energies of the four hemes in the gas phase and in proteins

Heme	c-559	c-556	c-554	c-552
ΔE (HOMO–LUMO) (eV)				
Gas phase	5.48	5.49	5.32	4.88
Proteins	6.37	6.43	6.54	4.85
Excitation energy (eV) (Oscillator strength)				
Gas phase				
2^1A	2.45 (0.014)	2.26 (0.034)	2.40 (0.036)	1.53 (0.160)
3^1A	2.55 (10^{-4})	2.30 (0.022)	2.52 (0.002)	1.82 (0.013)
4^1A	2.56 (0.006)	2.63 (10^{-5})	2.75 (10^{-6})	1.88 (0.003)
5^1A				2.40 (10^{-4})
6^1A				2.26 (0.150)
7^1A				2.88 (0.022)
Proteins				
2^1A	2.44 (0.057)	2.23 (0.047)	2.38 (0.035)	1.50 (0.124)
3^1A	2.51 (0.002)	2.27 (0.020)	2.51 (0.001)	1.83 (0.110)
4^1A	2.67 (10^{-4})	2.59 (10^{-6})	2.75 (10^{-5})	1.87 (0.001)
5^1A				2.40 (0.002)
6^1A				2.44 (0.059)
7^1A				2.71 (0.005)

Table 3. Excited states of c-552 calculated by the SAC-CI method in the gas phase and in the protein and water environment

State	Main configuration[a]	Nature	Excitation energy (eV)		Oscillator strength	LD/A		
			Calc.	Exptl		Calc.	Exptl	LD
Gas phase								
2^1A	0.676(128–130)−0.551(129–130)	por(π)–por(π)	1.53		0.1600			
3^1A	0.707(129–130)−0.618(128–130)−0.274(128–131)	por(π)–por(π)	1.82		0.0133			
4^1A	0.396(111–159)−0.385(111–152)		1.88		2.94×10^{-3}			
5^1A	−0.319(110–157)−0.296(110–152)−0.266(110–154)		2.40		8.30×10^{-4}			
6^1A	−0.842(127–130)−0.311(126–130)−0.260(129–131)	Im(π)+por(π)–por(π)	2.46		0.1500			
7^1A	0.266(110–157) + 0.251(118–157)		2.88		0.0133			
8^1A	0.183(110–159)−0.179(128–142)		4.07		0.0223			
Proteins								
2^1A	−0.658(128–130) + 0.574(129–130)	por(π)–por(π)	1.50	1.46	0.1243	−1.143	–	−2.990
3^1A	0.683(129–130) + 0.555(128–130)−0.262(128–131)	por(π)–por(π)	1.83	1.75, 1.81	0.1101	−1.349	–	−3.130
4^1A	−0.537(111–160)−0.468(111–154) + 0.265(111–152)		1.87		1.20×10^{-3}			
5^1A	−0.411(110–158) + 0.296(110–154)−0.255(110–153)		2.40		2.04×10^{-3}			
6^1A	0.768(127–130) + 0.471(126–130)		2.44	2.270	0.0588	−0.224	[b]	−0.708
7^1A	−0.353(116–158)−0.222(110–158) + 0.282(119–165)−0.275(119–165)		2.71		4.70×10^{-3}			
8^1A	0.619(124–130) + 0.561(129–131)		3.22		0.6214			

[a] (N–M) denotes the configuration due to excitation from MO N to MO M.
[b] Experimental LD/A value is difficult to estimate quantitatively since absorption peaks overlap with each other in this region.

Table 4. Excited states of c-554 calculated by the SAC-CI method in the gas phase and in the protein and water environment

State	Main configuration[a]	Nature	Excitation energy (eV)		Oscillator strength	LD/A		
			Calc.	Exptl		Calc.	Exptl	LD
Gas phase								
2^1A	0.799(128–129)−0.496(127–130)	por(π)–por(π)	2.40		0.03647			
3^1A	−0.717(128–130)−0.618(127–129)	por(π)–por(π)	2.52		1.53×10^{-3}			
4^1A	0.364(117–169) 0.359(117–153)−0.351(117–162)−0.294(117–161)		2.75		2.24×10^{-6}			
5^1A			2.87		0.98×10^{-4}			
6^1A			2.93		0.19×10^{-3}			
7^1A	−0.474(117–152) + 0.287(117–162) + 0.282(117–163)−0.275(117–163)		4.23		1.36×10^{-3}			
8^1A	−0.781(126–129)−0.310(125–129)−0.212(126–130)	por(π)–por(π)	4.64		0.04849			
Proteins								
2^1A	0.796(128–129)−0.502(127–130)	por(π)–por(π)	2.38	2.555	0.03470	−0.540	−0.54 + 0.05	−0.395
3^1A	−0.714(128–130)−0.616(127–129)	por(π)–por(π)	2.51		1.23×10^{-3}			
4^1A	−0.452(127–165) + 0.368(127–158) + 0.301(127–162)		2.75		7.80×10^{-6}			
5^1A	−0.243(110–153) + 0.219(118–153)		2.83		4.43×10^{-5}			
6^1A	0.198(111–153)−0.169(115–153) + 0.162(118–153)		2.99		0.19×10^{-3}			
7^1A	−0.471(117–153) + 0.267(117–161) + 0.282(117–163 − 0.275(117–163)		4.26		7.78×10^{-3}			
8^1A	−0.788(125–129) + 0.191(125–129)		4.43		0.12267			

[a] (N–M) denotes configuration due to excitation from MO N to MO M.

Table 5. Excited states of c-556 calculated by the SAC-CI method in the gas phase and in the protein and water environment

State	Main configuration[a]	Nature	Excitation energy (eV)		Oscillator strength	LD/A		LD
			Calc.	Exptl		Calc.	Exptl	
Gas phase								
2^1A	−0.733(128–129)−0.452(127–130)−0.338(128–130)	por(π)–por(π)	2.26		0.0339			
3^1A	−0.715(128–130) + 0.477(127–129) + 0.347(128–129)	por(π)–por(π)	2.30		0.0226			
4^1A	−0.564(116–162) + 0.403(116–154)−0.321(116–169)		2.63		2.56×10^{-5}			
5^1A	−0.245(111–162)−0.239(111–152)		2.73		5.53×10^{-5}			
6^1A	0.233(110–163)−0.225(118–163)		3.14		4.35×10^{-4}			
7^1A	−0.771(127–129)−0.474(128–130)		3.78		1.2126			
8^1A	0.471(125–129)−0.331(116–152) + 0.329(116–163)−0.300(126–129)		4.26		7.30×10^{-3}			
Proteins								
2^1A	−0.578(128–129)−0.417(127–130)	por(π)–por(π)	2.23	2.233	0.0473	−0.675	−0.60 + 0.05	−0.675
3^1A	−0.711(128–130) + 0.494(127–129)	por(π)–por(π)	2.27	2.249	0.0199	+0.445	+0.80 + 0.05	+0.708
4^1A	−0.534(116–161) + 0.352(116–168)−0.317(116–152)		2.59		6.47×10^{-6}			
5^1A	0.235(115–152) + 0.235(115–151)		2.72		2.95×10^{-5}			
6^1A	−0.209(115–161) + 0.207(112–151)		2.84		6.67×10^{-4}			
7^1A	−0.757(127–129)−0.493(128–130)		3.72		1.1899			
8^1A	0.376(116–151)−0.297(124–129) + 0.293(116–152)		4.19		7.14×10^{-4}			

[a] (N–M) denotes configuration due to excitation from MO N to MO M.

Table 6. Excited states of c-559 calculated by the SAC-CI method in the gas phase and in the protein and water environment

State	Main configuration	Nature	Excitation energy (eV)		Oscillator strength	LD/A		LD
			Calc.	Exptl		Calc.	Exptl	
Gas phase								
2^1A	−0.749(128–129)−0.532(127–130)	por(π)–por(π)	2.45		0.0135			
3^1A	0.453(127–154) + 0.350(117–168)−0.348(117–162)	por(π)–por(π)	2.55		7.89×10^{-5}			
4^1A	0.723(128–130)−0.559(127–129)		2.56		5.75×10^{-3}			
5^1A	0.330(110–152) + 0.235(116–152)		3.06		1.38×10^{-5}			
6^1A	0.394(115–152)−0.265(118–152)		3.16		1.27×10^{-4}			
7^1A	−0.725(127–129)−0.474(128–130)		4.01		1.4415			
8^1A	−0.268(115–152) + 0.259(115–154)		4.75		7.16×10^{-4}			
Proteins								
2^1A	0.808(128–129) + 0.446(127–130)	por(π)–por(π)	2.44	2.225	0.0575	+0.509	−0.60 + 0.03	0.617
3^1A	0.700(128–130)−0.606(127–129)	por(π)–por(π)	2.51		1.81×10^{-3}	+000.4		$+1.70 \times 10^{-4}$
4^1A	−0.437(117–157)−0.373(117–158) + 0.367(117–164)		2.67		1.03×10^{-4}			
5^1A	0.363(115–153) + 0.283(110–153)		2.84		3.27×10^{-5}			
6^1A	0.307(115–153) + 0.265(115–157) + 0.258(118–153)		2.99		2.53×10^{-5}			
7^1A	−0.797(127–130) + 0.421(128–129)		3.95		1.1830			
8^1A	0.726(126–129)−0.316(117–153)		4.34		0.0279			

[a] (N–M) denotes configuration due to the excitation from MO N to MO M.

main configurations and oscillator strengths of four hemes in the PSRC of *Rps. viridis*, calculated by the SAC-CI method. The results in the gas phase are listed in the upper half of the tables, and those in the protein and water environment in the lower half.

The four hemes in the present study were identified by the wavenumbers of the α-absorption band, and therefore these wavenumbers are the origin of the names of the four hemes, c-559, c-556, c-554, and c-552, as described above. As seen in Table 2, the HOMO–LUMO energy separations of c-559, c-556, and c-554 parallel with the excitation energies of these hemes, and these excitations have oscillator strengths at a similar magnitude (0.035–0.057 in proteins). On the other hand, the lowest excited state of c-552 was much more stable (1.50 eV) than those of the other hemes, and oscillator strength was five times stronger. The 6^1A state of c-552 was located at 2.44 eV and had an oscillator strength of 0.059, which was comparable with the lowest states of c-559, c-556, and c-554, though the nature of this state was different from those of the other hemes. Keeping this fact in mind, we discuss below the excited states of the four hemes.

We discuss first the lowest and the second lowest excited states. The excitation energies of these states are shown in Tables 3–6, and summarized in Table 2. The lowest two excited states of c-559, c-556, and c-554 are well described by Gouterman's four-orbital model [40]. Namely, the lowest excited state consists of transitions from the HOMO to the LUMO and from the next HOMO to the next LUMO, while the second lowest state consists of those from the next HOMO to the LUMO and from the HOMO to the next LUMO. As we reported previously [16], oscillator strengths became weak since the transition dipole moments cancel in these two configurations. The excited states of c-552 (at 1.50 eV and 1.83 eV) are much more stable than those of the other hemes, as predicted by the HOMO–LUMO energy separations in Table 2. These states consist of the transitions from the next HOMO and the HOMO to the LUMO, since the next LUMO of c-552 is much higher in energy than the LUMO (see Fig. 2). Thus, the cancellation of the transition dipole moments does not occur, and the oscillator strength of the 1^1A state of c-552 is relatively large, as shown in Table 2.

Next we examine some other states which have moderately large oscillator strengths. They include porphyrin-π-orbitals, 3d orbitals of Fe, and ligand orbitals. In c-554 8^1A (4.43 eV) includes metal–porphyrin transition; in c-556, 7^1A (3.72 eV) porphyrin–porphyrin transition; in c-552, 6^1A (2.44 eV) imidazole–porphyrin transition and 8^1A (3.22 eV) porphyrin–porphyrin transition; in c-559, 7^1A (3.95 eV) porphyrin–porphyrin transition, and 8^1A (4.34 eV) porphyrin–porphyrin and small metal–porphyrin transitions. This variety is due to both the ligand and environmental effects. The excitation energy of the 6^1A (2.44 eV) state of c-552 is located in the same energy region of the lowest excited states of the other hemes.

As mentioned above, the names of c-559, c-556, c-554, and c-552 are taken from the wavenumbers in the α-absorption peaks observed in the 550 nm region. The 2^1A states of c-556 and c-554 and the 3^1A state of c-556 are located in this energy region and have relatively large oscillator strength, and the 6^1A state of c-552 is also located close to this region, having a similar oscillator strength when it is in protein (the gas phase value is much larger). Though, unfortunately, the calculated values are not in the same trend as the observed wavenumbers, the assignment of these states is discussed in the next section.

Although the environmental effect on the excited states is generally small in comparison with the ligand effect, it provides closer agreement between the calculated and observed transition energies. We should note that, in c-559 only, the main configuration of the second lowest excited state is significantly modified by the environmental effect. Namely, only in proteins and waters, the lowest two excited states of c-559 clearly conform to Gouterman's four-orbital model. The environment effect of these four hemes is much smaller than that of bacteriochlorophyll and bacteriopheophytin which we calculated previously [18, 19].

ASSIGNMENT OF THE UV AND CIRCULAR DICHROISM (CD) SPECTRA

In our previous report [18, 19], all peaks in the UV absorption spectrum of the PSRC of *Rps. viridis* were assigned by SAC-CI calculations for all chromophores and hemes in the environment of proteins and waters of the PSRC. The assignments are shown in Tables 3–6. Absorption bands I–XVI in the spectrum of the PSRC are shown in Fig. 6 of the previous report [19].

The second band II observed at 1.46 eV is assigned to the 2^1A state of c-552 and the second lowest excited state of a special pair [19]. This peak vanishes in the oxidized PSRC, which is reasonable since the hemes are oxidized in the oxidized PSRC. The excitation energy of the 2^1A state of c-552 of 1.53 eV, the oscillator strength of 0.124, and the LD angle of 43.3° are consistent with the nature of band II. Band VII observed at 1.81 eV is assigned to the 3^1A state of c-552 which is calculated at 1.83 eV. Only c-552 has excited states in this low-energy region, while the other hemes have no electronic states in such a low-energy region.

Band VIII at about 1.99 eV is assigned to the 2^1A state of c-556, which is calculated at 2.23 eV of having an LD angle of 44.6°. Another possibility for this assignment exists, as reported previously [18, 19]. Band XVI at about 2.36–2.38 eV was assigned to the 2^1A state of c-554 and the 6^1A state of c-552. The 2^1A states of c-559 may also belong to band XVI.

CONCLUSION

The excited states of four hemes, c-559, c-556, c-554, and c552, in the PSRC of *Rps. viridis* were calculated by the SAC-CI method, including the effect of the environment of proteins and other chromophores.

Ligand Effect

c-552 has two imidazole ligands and the other hemes c-559, c-556, and c-554 have imidazole and methionine. This classifies four hemes into two groups, one c-552 and the other c-559, c-556, and c-554.

In comparison with free-base porphin [9] and Mg porphin [11], the natures of the HOMO and the next HOMO are exchanged in c-559, c-556, and c-554, while those in c-552 remain the same.

The HOMO–LUMO energy separation of c-552 is much smaller than that of the other hemes.

Gouterman's four-orbital model is upheld in c-559, c556, and c-554, but cannot be applied to c-552.

Excitation energies of the low-lying states of c-552 are much smaller than those of the other hemes.

Environmental Effect

The four hemes are surrounded by the unique environment of proteins and waters. This affects the electronic states of each heme.

The environmental effects lead to the fact that Gouterman's four-orbital model cannot be applied in c-552. The oscillator strength of the 6^1A state of c-552 also becomes weaker.

The nature of some low-lying excited states and their oscillator strengths of c-559 are significantly modified by the environmental effect.

Assignment

As reported in previous papers [18, 19], absorption peaks at 1.46 eV (II) and 1.81 eV (VII) of the PSRC are assigned to the lowest and the second-lowest excited states of c-552 (1.50 eV and 1.83 eV). The absorption peaks at 2.36–2.38 eV (XVI) are also assigned to the lowest excited states of c-554 and c-559, and to the 6^1A state of c-552. The peak at 1.99 eV (VIII) is assigned to the first excited state of c-556. The calculated linear dichroism (LD) angles are consistent with the observed ones, supporting the above assignment.

Acknowledgement

This work was supported by a Grant-in-Aid for Scientific Research from the Japanese Ministry of Education, Science, Culture, and Sports.

REFERENCES

1. Deisenhofer J, Epp O, Miki K, Huber R, Michel H. *J. Mol. Biol.* 1984; **180**: 385.
2. Voet D, Voet JG. *Biochemistry*, 2nd ed. Wiley: New York, 1995; chap. 22.
3. Andre V, Pierre R, and Jacques B. *FEBS Letters*, 1989; **243**: 259.
4. Kaminskaya O, Konstantiov AA, and Shuvalov VA. *Biochim. Biophys. Acta* 1990; **1016**: 153.
5. Alegria G, and Dutton L. *Biochim. Biophys. Acta* 1991; **1057**: 258.
6. Fritzsh G, Buchanan S, and Michel H. *Biochim. Biophys. Acta* 1989; **977**: 157.
7. Nitschke W, and Rutherfold AW. *Biochemistry* 1989; **28**: 3161.
8. Dracheva SM, Drachev LA, Zaberezhnaya SM, Konstantinov AA, Semenov AY, and Skulachev VP. *FEBS Lett.* 1986; **205**: 41.
9. Nakatsuji H, Hasegawa J, Hada M. *J. Chem. Phys.* 1996; **104**: 2321.
10. Tokita Y, Hasegawa J, Nakatsuji H. *J. Phys. Chem. A* 1998; **102**: 1843.
11. Hasegawa J, Hada M, Nonoguchi M, and Nakatsuji H. *Chem. Phys. Lett.* 1996; **250**: 159.
12. Hasegawa J, Ozeki Y, Ohkawa K, Hada M, and Nakatsuji H. *J. Phys. Chem. B* 1998; **102**: 1320.
13. Nakatsuji H, Tokita Y, Hasegawa J, Hada M. *Chem. Phys. Lett.* 1996; **256**: 220.
14. Nakatsuji H, Hasegawa J, Ueda H, Hada M. *Chem. Phys. Lett.* 1996; **250**: 379.
15. Toyota K, Hasegawa J, and Nakatsuji H. *Chem. Phys. Lett.* 1996; **250**: 437.
16. Tokita Y, and Nakatsuji H. *J. Phys. Chem. B* 1997; **101**: 3281.
17. Toyota K, Hasegawa J, Nakatsuji H. *J. Phys. Chem. A* 1997; **101**: 446.
18. Nakatsuji H, Hasegawa J, Ohkawa K. *Chem. Phys. Lett.* 1998; **296**: 499.
19. Hasegawa J, Ohkawa K, and Nakatsuji H. *J. Phys. Chem. B* 1998; **102**: 10 410.
20. Hasegawa J, and Nakatsuji H. *J. Phys. Chem. B* 1998; **102**: 10 420.
21. Nakatsuji H, and Hirao K. *J. Chem. Phys.* 1978; **68**: 2053.
22. Nakatsuji H. *Chem. Phys. Lett.* 1978; **59**: 362.
23. Nakatsuji H. *Chem. Phys. Lett.* 1979; **67**: 329.
24. Nakatsuji H. *Chem. Phys. Lett.* 1979; **67**: 334.
25. Nakatsuji H. *Acta Chim. Hung.* 1992; **129**: 719.
26. Nakatsuji H. In *Computational Chemistry Reviews of Current Trends*, Vol. 2. Leszczynski J. (ed). World Scientific: Singapore, 1996; 62–124.
27. Breton J. *Biochim. Biophys. Acta* 1985; **810**: 235.
28. Abola EE, Bernstein FC, Bryant SH, Koetzle TF, Weng J. Protein Data Bank, in *Crystallographic Databases-Information Content, Software Systems, Scientific Applications*; Allen FH, Bergerhoff G, Sievers R. Eds., Data Commission of the International Union of Crystallography, Chester, 1987, pp 107–132.
29. Bernstein FC, Koetzle TF, Williams GJB, Meyer EF Jr.,, Brice MD, Rodgers JR, Kennard O, Shimanouchi T, Tasumi M. The protein data bank, a computer-based archival file for macromolecular structures. *J. Mol. Biol.* 1977; **112**: 535.
30. SYBYL, Version 6.1, TRIPOS Inc., St. Louis, Missouri.
31. Huzinaga S, Andzelm J, Klobukowski M, Radzio-Andzelm E, Sakai Y, Tatewaki H. *Gaussian Basis Set for Molecular Calculations*, Elsevier, New York, 1984.
32. Huzinaga S. *J. Chem. Phys.* 1965; **42**: 1293.
33. Cornell WD, Cieplak P, Bayly CI, Gould IR, Merz KM, Ferguson DR, Spellmeyer DC, Fox T, Caldwell JW, and Kollman PA. *J. Am. Chem. Soc.* 1995; **117**: 5197.
34. Jorgensen WL, Chandrasekhar J, Madura JD, Impey RW, and Klein ML. *J. Chem. Phys.* 1983; **79**: 926.
35. Dupuis M, Farazdel A. MOTECC-91, Center of Scientific and Engineering Computations, IBM Corporation, 1991.
36. Nakatsuji H, Hada M, Ehara M, Hasegawa J, Nakajima T, Nakai H, Kitao O, Toyota K. SAC/SAC-CI program system (SAC-CI96) for calculating ground, excited, ionized, and electron attached states and singlet to Septet Spin Multiplicities, 1998, to be submitted for publication.
37. Nakatsuji H. Program System for SAC and SAC-CI Calculations, Program Library No. 146 (Y4/SAC), Data Processing Center of Kyoto University, Kyoto Japan, 1985.
38. Nakatsuji H. Program Library SAC85, No. 1396, Computer Center of the Institute of Molecular Science, Okazaki, 1981.
39. Parson WW, Warshel A. *J. Am. Chem. Soc.* 1987; **109**: 6152.
40. Gouterman M. *The Porphyrins*, Vol. 3, ed. by D. Dolphin, Academic Press, New York, 1977.